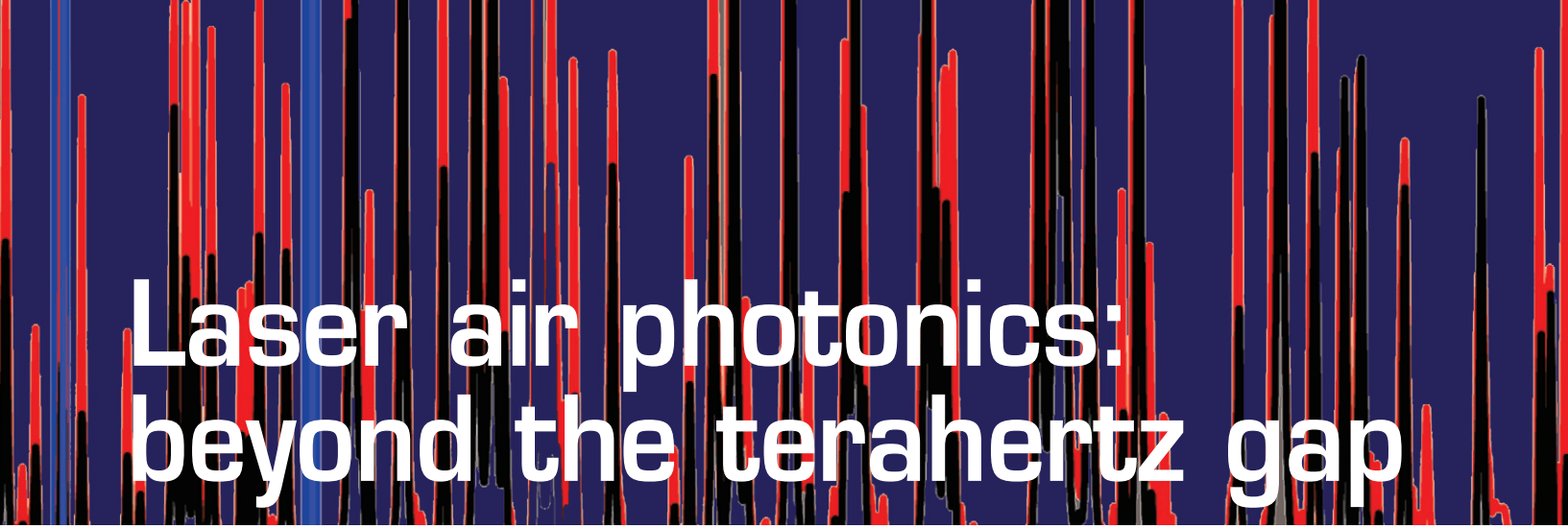

Laser air photonics: beyond the terahertz gap

Through the ionization process, the very air that we breath is capable of generating terahertz (THz) electromagnetic field strengths greater than 1 MV/cm, useful bandwidths of over 100 THz, and highly directional emission patterns. Following the ionization of air, the emitted air-plasma fluorescence or acoustics can serve as an omnidirectional, broadband, THz wave sensor. Here we review significant advances in laser air photonics that help to close the "THz gap," enabling ultra-broadband THz wave generation and detection, for applications including materials characterization and non-destructive evaluation. The feasibility for remote sensing, as well as the remaining challenges and future opportunities are also discussed.

Benjamin Clough[a,b], Jianming Dai[a,b,c], and Xi-Cheng Zhang*[a,b,c]

[a]Huazhong University of Science and Technology, 1037 Luoyu Road, Wuhan 430074, China

[b]Center for Terahertz Research, Rensselaer Polytechnic Institute, Troy, New York 12180, USA

[c]The Institute of Optics, University of Rochester, Rochester, New York 14627, USA

**E-mail: Corresponding author: zhangxc@rpi.edu*

Plasma is regarded as the fourth state of matter[1] because it exhibits unique characteristics that set it apart from solids, liquids, and gases. A bolt of lightning, the glow of the Northern Lights, and the light of stars all stem from plasma formation. When a laser pulse is focused into a gas with intensity above a critical value near 10^{14} W/cm^2, the gas is ionized, yielding positively and negatively charged particles, or plasma[2]. High-energy pulsed lasers capable of ionizing ambient air or select gases were once only available at large-scale scientific facilities. Although pulsed CO_2 lasers capable of ionizing air have been in use since the 1970s, the optical pulse durations were insufficiently short for terahertz (THz) wave generation. Frequencies lying within the THz band were historically termed the "THz gap," due to the relative difficulty of generating and detecting the radiation at these frequencies. More recent advancements in laser technologies have included self-mode-locked femtosecond Ti:sapphire oscillators, based on the Kerr effect, and high-power femtosecond Ti:sapphire amplified laser systems, based on chirped pulse amplification (CPA)[3]. These technologies have allowed for critical intensities with pulse durations on the order of femtoseconds in commercial tabletop laser systems. This has substantially increased the interest in using laser air photonics within the THz science community.

Laser-induced gas-plasma can be used to generate intense, coherent, broadband, and highly directional THz waves through a nonlinear optical process[4-10]. Moreover, plasma in ambient air or other selected gases can be used as a THz wave sensor[11-16]. One technique, termed THz air biased coherent detection (THz-ABCD)[11-12], provides superior bandwidth (0.1 to 40 THz), detection sensitivity (using the heterodyne method), and frequency resolution (MHz). These parameters are important for the

ISSN:1369 7021 © Elsevier Ltd 2012

study of materials since many non-metallic molecular compounds exhibit vibrational and rotational resonances when stimulated by THz waves. Therefore, THz radiation can serve as a unique tool for non-invasive material classification, particularly since it easily penetrates many optically opaque materials such as paper, plastics, and clothing. By detecting THz radiation after its interaction with a material, absorption features at the resonant frequencies can be used as a unique spectral signature, or "fingerprint," for its identification. It is clear that air photonics presents a unique technique for the generation and detection of THz radiation, but it remains desirable to seek sensing methods which could apply this powerful technology while overcoming existing limitations such as stand-off distance and limited detection geometries.

Plasma formed in gas through laser-atom/molecule interaction emits both fluorescence and acoustic waves. When the plasma is subject to a strong external electric field, both the intensity of fluorescence amplitude of the acoustic waves are increased by the transfer of kinetic energy from accelerated electrons to surrounding molecules through electron-electron, electron-ion, and electron-neutral atom collisions. THz radiation enhanced emission of fluorescence (THz-REEF) and THz enhanced acoustics (TEA)[13-18], are two techniques that utilize a dual-color laser field (800 and 400 nm pulses of light superimposed in space and time) to create air-plasma with asymmetric electron motion, making it possible to coherently detect broadband THz waves remotely. Amplitude and phase information obtained from the THz wave, can be used for performing THz spectroscopy of materials. These techniques can overcome large THz wave absorption by water vapor in air, and limited detection angles, by carrying THz wave information in the form of fluorescence or acoustic waves that are emitted in an isotropic manner.

The basic science and engineering of laser air photonics for wideband, high-field THz technology is just beginning. Here we review THz wave generation and detection techniques, sensing methodologies, applications for material classification, remaining challenges, and future opportunities for this rapidly evolving area of research that transcends the "gap" once existing between optics and electronics.

Generation and detection of terahertz waves in air

THz wave generation from intense laser-plasma interaction in air was first reported by Hamster *et al.* in 1993[4]. At the time, single color (800 nm) sub-picosecond laser pulses were used, and the generation process was attributed to the ponderomotive force inside the plasma. In 2000, Cook *et al.* reported that higher intensity THz radiation could be emitted from laser-induced gas-plasma excited with both a fundamental pulse (800 nm) and its second harmonic (400 nm)[5]. The THz wave emission mechanism was attributed to the four-wave mixing (FWM) nonlinear optical process. At that time, several other groups became interested in this topic. Among them, Bartel *et al.* reported THz wave generation from gas-plasma with peak electric fields higher than 100 kV/cm, indicating promising applications of the gas-plasma THz wave source[6]. However,

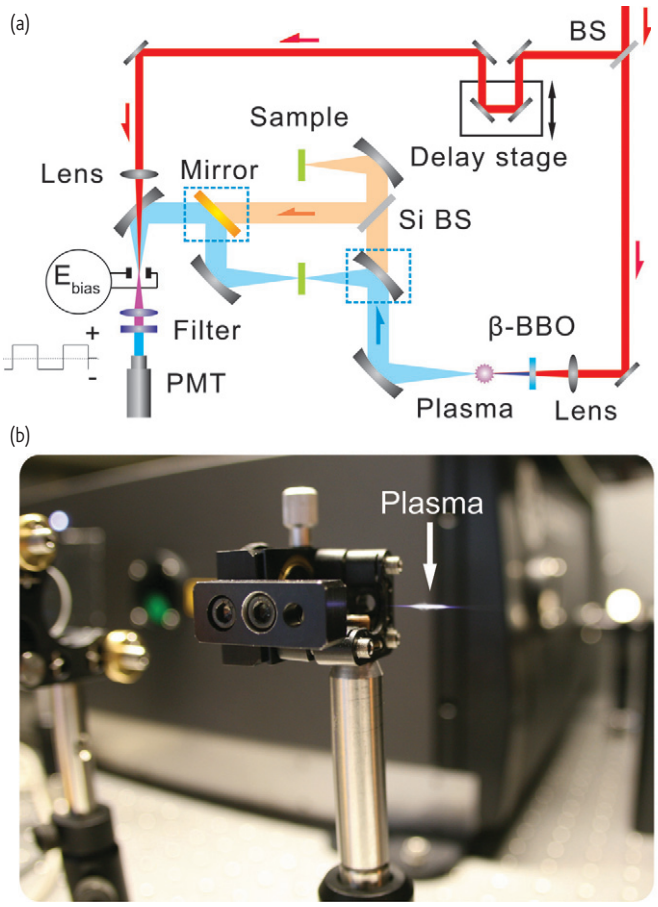

Fig. 1 (a) Schematic diagram of a THz-ABCD spectroscopic system in both transmission and reflection mode. The system can be converted from transmission to reflection mode by taking off the mirrors indicated with an enclosing dashed box. (b) Photograph of laser-induced air-plasma created after focusing the optical beam from left to right through a lens (left) and mounted nonlinear crystal (center) used for second harmonic generation. The bright horizontal line emits an intense, highly directional THz field to the right. PMT: photomultiplier tube; BS: beamsplitter; β-BBO: beta-barium borate.

the physical process for THz wave emission remained under debate. In order to identify the basic mechanism, coherent control experiments were performed which verified that FWM could be used to explain the THz wave generation process in a gas-plasma[19]. More importantly, using the FWM approximation, the detection of broadband pulsed THz waves with a laser-induced gas-plasma was successfully predicted and experimentally demonstrated[11]. In light of this, THz wave generation and detection with laser-induced gas-plasma have become attractive scientific research topics, and many groups worldwide have become involved[6-9,14-15,20-29].

Laser air photonic systems differentiate themselves from other THz time-domain spectrometers by using ambient air or selected gases for the generation and detection of broadband pulsed THz waves[19,30-32]. Fig. 1a illustrates the schematic diagram for a THz-ABCD spectroscopic system in both transmission and reflection mode.

A Ti:sapphire regenerative amplifier is used as the laser source. Such a laser typically delivers laser pulses with millijoule pulse energy,

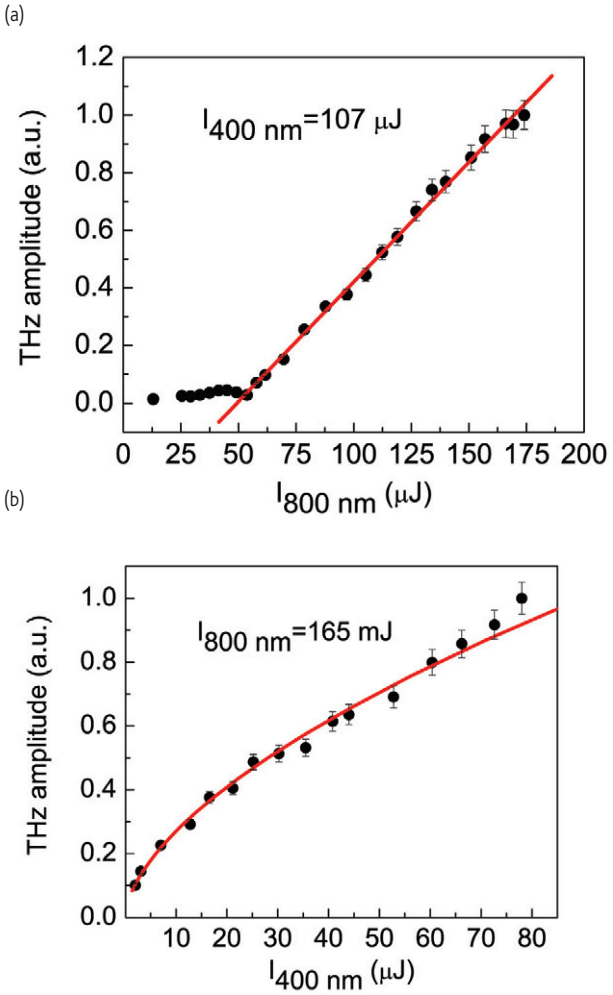

Fig. 2 (a) Dependence of THz field on fundamental (ω) pulse energy, with fixed second-harmonic (2ω) pulse energy. (b) Dependence of THz field on second-harmonic pulse energy, with fixed fundamental pulse energy. The solid line and curve are the linear and square-root fits, respectively. Reprinted figure with permission from[59]. © 2006 by the American Physical Society.

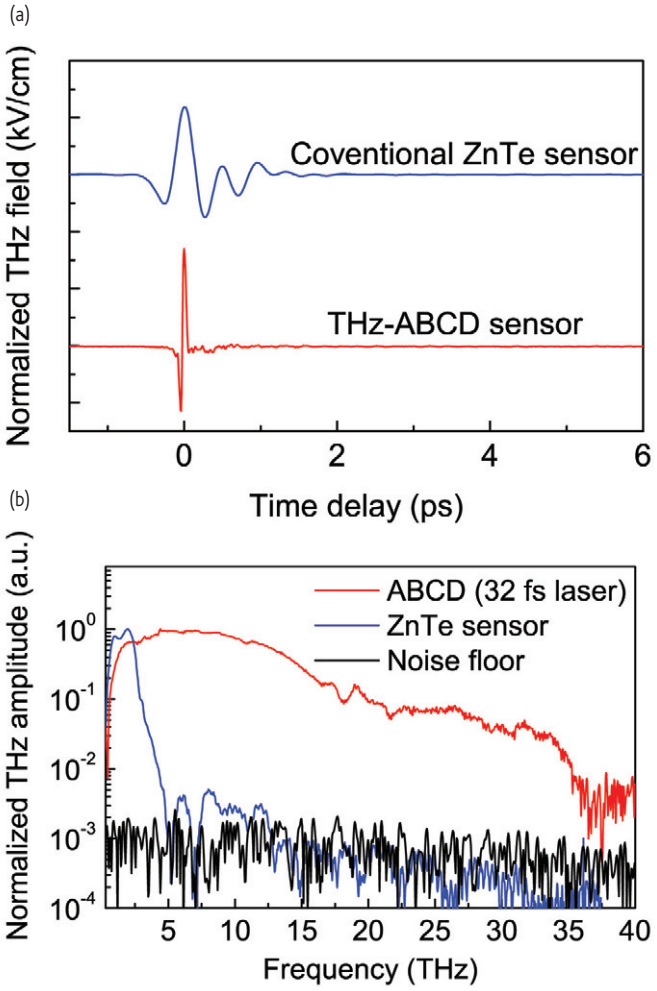

Fig. 3 (a) Time-resolved THz signals generated and detected using dry nitrogen gas as compared to conventional EO crystal detection in ZnTe. The probe beam for air detection has energy of 85 μJ and pulse duration of 32 fs. (b) Corresponding spectra after Fourier transform.

femtosecond pulse duration, 800 nm center wavelength, and kilohertz repetition rate. The beam is split into pump and probe beams using a beamsplitter. The pump beam is focused through a beta-barium borate (β-BBO) crystal to produce the second harmonic at 400 nm. The mixed fundamental and second harmonic beams (ω and 2ω respectively) generate the ionizing plasma spot (center-right of Fig. 1b) that emits intense, directional, and ultra-broadband THz radiation through a third-order nonlinear process[5]. Although four-wave-mixing (FWM) cannot completely describe the complex physical details[33-36], it remains a convenient framework for experimental results due to its simplicity. After interaction with a sample, the remaining THz energy and optical probe beam are recombined at the detection region, where an electric bias (E_{bias}) is applied to create a second harmonic local oscillator for coherent detection through DC-field-induced second harmonic generation[12]. Fig. 2 shows that the THz field is proportional to the intensity of the fundamental pulse (ω) above the ionization threshold for lower intensities, and is proportional to the square root of the second harmonic pulse (2ω)[37]:

$$E_{THz} \propto \chi^{(3)} \sqrt{I_{2\omega}} I_{\omega} \quad (1)$$

It is important to note that this relationship is only valid for relatively low peak laser power intensities, since FWM is an approximation in the perturbation region that is no longer valid when the laser intensity is very high.

Similar to the widely used generation and detection of THz waves in electro-optic (EO) crystals by second-order optical nonlinearity[38-40], THz waves can be detected by the third-order optical nonlinearity in air or other selected gases[11,31]. Figs. 3a,b plot THz waveforms and spectra detected with laser-induced air-plasma using THz air-biased coherent

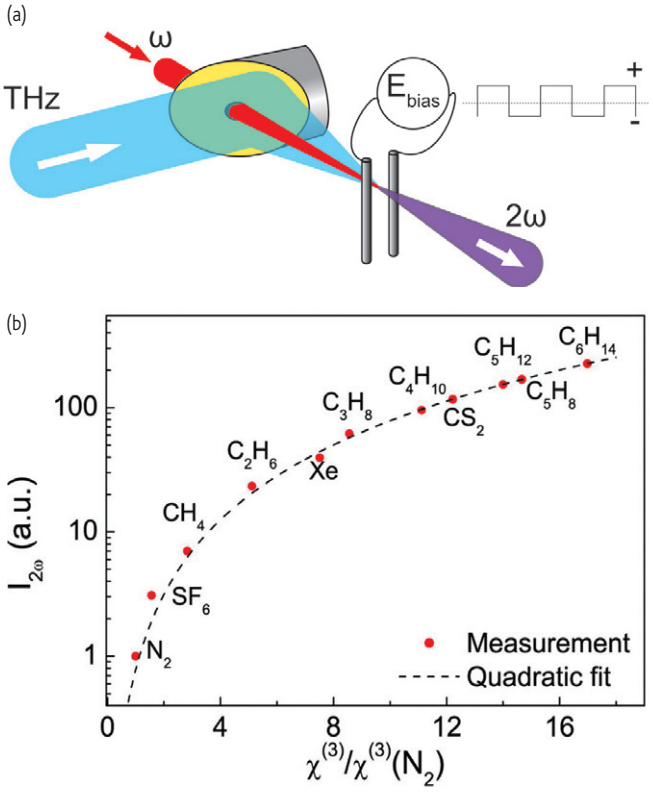

Fig. 4 (a) Basic concept of THz-ABCD: electrodes are placed at the geometric focus of collinearly focused THz and optical probe beams with a variable time delay. Second harmonic light is induced from the THz field and the local bias field E_{bias}. Modulating E_{bias} allows for heterodyne detection for enhanced sensitivity. (b) Measured second harmonic intensity vs third order nonlinear susceptibility $c^{(3)}$. All $c^{(3)}$ are normalized with respect to nitrogen.

detection (THz-ABCD) in comparison with the conventional EO method with a ZnTe crystal as the sensor. Using air as the sensor, the spectrum from 0.3 THz to over 30 THz sufficiently covers the "THz gap". Using shorter laser pulses, THz peak fields may exceed 1 MV/cm, and the spectrum may extend beyond 120 THz[41]. As a comparison, the DC breakdown threshold for air is about 30 kV/cm.

The use of air to sense pulsed THz waves is a measurement of the THz field induced optical second harmonic light generated through a third-order nonlinear process that has been investigated extensively in the previous literature[12,42-43], and therefore details will not be presented here. The measured second harmonic intensity can be expressed as:

$$I_{2\omega}(\tau) \propto 2\left[\chi^{(3)} I_{\omega}(t)\right]^2 E_{bias}\, E_{THz}(t-\tau) \qquad (2)$$

Eq. 2 is the key description for detection. The linear dependence of $I_{2\omega}$ on E_{bias} indicates heterodyne detection when E_{bias} is treated as a local oscillator. The field induced second harmonic signal $I_{2\omega}$ is quadratically proportional to $\chi^{(3)}$ and $I_{\omega}(t)$, and linearly proportional to E_{bias} and $E_{THz}(t-\tau)$. Fig. 4a illustrates this concept where THz and optical pulses are focused together between modulated high-voltage-biased electrodes. The second harmonic induced by E_{bias}acts as the local oscillator for heterodyne detection[12]. Fig. 4b plots the detected second harmonic intensity as a function of normalized third order nonlinear susceptibility $\chi^{(3)}$ along with a quadratic fit[31,44]. C_6H_{14} provides more than 243 times the sensitivity compared with N_2 or air. Using gases with larger $\chi^{(3)}$, elevated pressure (effective $\chi^{(3)}$ is proportional to the number of molecules), and higher probe pulse energy can help to optimize the sensitivity of the air-plasma detector[31].

THz sensing with air-plasma: fluorescence & acoustics

Intense, broadband, pulsed THz wave generation is achieved at remote locations by focusing two-color laser pulses into air at distances of tens of meters or even potentially hundreds of meters[29,45-46] away. THz signals can be detected indirectly by observing THz radiation enhanced emission of fluorescence (THz-REEF), or THz enhanced acoustics (TEA). The THz spectroscopic "fingerprints" of materials can thus be carried to the operator via fluorescence (wavelength of 300 – 450 nm), or acoustic frequencies (10 Hz – 140 kHz), due to their atmospheric transparencies. In the THz-REEF experiment, as shown in Fig. 5a, a THz pulse propagates through the plasma and the fluorescence is measured

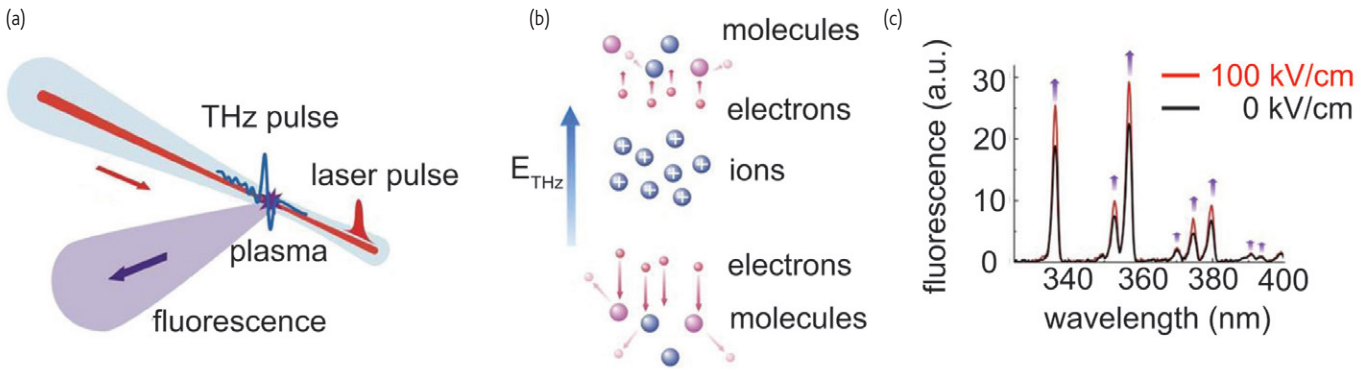

Fig. 5 (a) Experimental geometry for THz-REEF from air-plasma using a single-color laser pulse. (b) Electron acceleration in the THz field and collision with neighboring molecules. (c) THz-enhanced fluorescence spectra of nitrogen gas-plasma under influence of 100 kV/cm peak field. © IEEE, Reprinted, with permission, from[60].

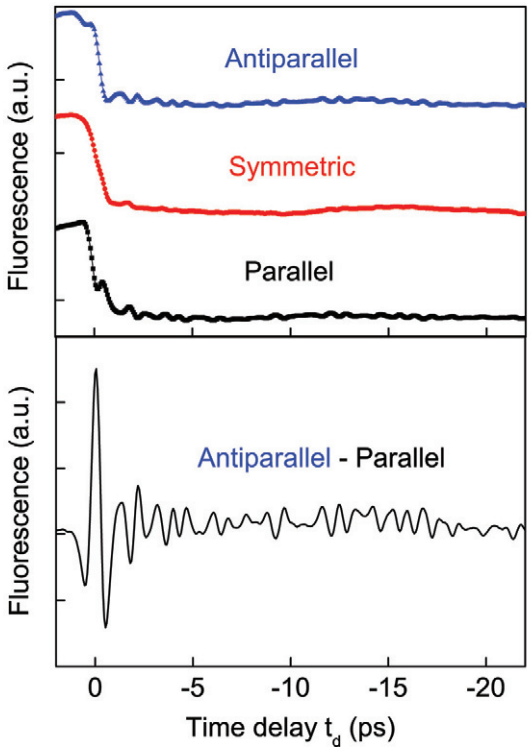

Fig. 6 Time-resolved air-plasma fluorescence enhancement from THz wave interaction with antiparallel, symmetric, and parallel electron drift velocities with respect to the laser field, controlled by changing the relative phase between the ω and 2ω optical pulses. Subtracting the parallel curve from the antiparallel curve removes the incoherent energy transfer by electrons after inelastic collisions and scattering at random directions. This reveals the THz waveform in the form of fluorescence modulation. The optical pulse leads the THz pulse in time for delay $t_d < 0$.

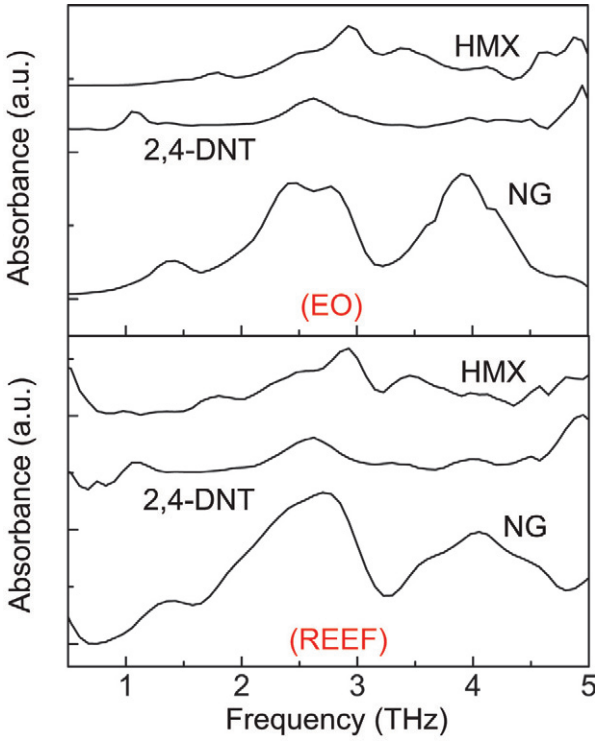

Fig. 7 (Top) Absorbance signatures for pellet samples of explosives: NG, 2,4-DNT, and HMX (20% in polyethylene) using conventional EO sampling. (Bottom) Absorbance signatures obtained using THz-REEF. All samples tested were in a transmission geometry and identical samples were used for the respective methods. Curves are offset for clarity.

by a spectrometer. By increasing the kinetic energy of electrons through THz-field acceleration in the plasma, as illustrated in Fig. 5b, fluorescence emission can be enhanced. Fig. 5c plots the nitrogen fluorescence spectra with and without THz field imposed on the gas-plasma.

When two-color pulses (800 nm and 400 nm) create a plasma, the ionized electrons' net drift velocity becomes a function of the relative phase between the pulses[34]. Electron motion can be symmetric, parallel, or anti-parallel to the THz wave polarization by changing the relative phase of the pulses. Once the THz pulse arrives, electrons are driven to move faster (if $E_{THz}(t)$ is anti-parallel to the initial velocity) or slower (if $E_{THz}(t)$ is parallel). The upper half of Fig. 6 shows the time-resolved air-plasma fluorescence for the parallel, symmetric, and antiparallel electron drift velocities as the THz pulse interacts with the plasma. In each scenario, there is fluorescence enhancement, but each contains unique "features" from either the increase or decrease in electron velocity (and therefore energy transfer) by the THz field[14]. The lower half of Fig. 6 shows the coherent THz waveform revealed in the fluorescence by subtracting the parallel curve from the antiparallel curve.

The THz-REEF signal thus allows for THz wave coherent detection, meaning air-plasma fluorescence can indirectly give information regarding a material. The omnidirectional nature of the fluorescence emission is a further advantage for THz wave detection. This method was demonstrated using air-plasma for both the THz wave emitter and detector[16]. THz-REEF has been used for sensing several explosive compounds in a transmission mode: nitroguanidine (NG), 2,4-dinitrotoluene (DNT), and octogen (HMX). Fig. 7 compares the absorbance information obtained using THz-REEF with that obtained using conventional EO sampling with ZnTe.

Although monitoring optical photons gives highly sensitive detection, UV from sunlight may easily saturate a sensitive photodetector such as a photomultiplier tube (PMT), making field measurements difficult. Therefore, it is useful to search for complementary sensing techniques.

A distinct acoustic pitch can be heard from laser-induced air-plasma as the gas is ionized at the repetition rate of the laser[47-48]. Although the main component of audible sound is determined by the repetition rate of the amplified laser (typically on the order of kHz), much like a repetitive clap of the hands, a very broad range of acoustic frequencies corresponding to high harmonics, are emitted for each clap. When a pulse of THz radiation is incident on the plasma, electrons are accelerated in the field and electron-electron, electron-ion, and electron-neutral atom collisions increase the gas temperature. Since an acoustic sound results from a variation in pressure, due to kinetic energy transfer from accelerated electrons to the

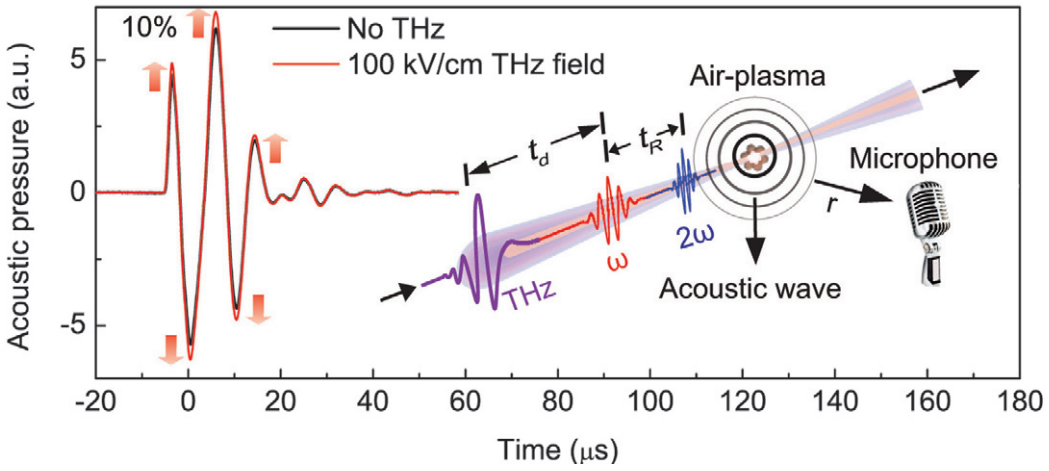

Fig. 8 Single acoustic pulse measured using a high frequency microphone from 10 mm radial distance when an 85 fs, 100 μJ optical pulse is focused into air with and without interaction with THz radiation. (Inset) Schematic of a THz-enhanced acoustics (TEA) measurement. A pulsed laser and its second harmonic generate an air-plasma which releases acoustic waves that are enhanced under the influence of THz radiation. A microphone detects the amplitude changes in these pressure waves.

gas-plasma, excess heating serves to change the air pressure, resulting in sound amplification under the influence of THz radiation. For this reason, a THz wave can be "heard" using a microphone.

Fig. 8 shows acoustic pulses formed by focusing an 85 fs optical pulse into air. The acoustic pressure is enhanced by 10 % for an incident peak field of 100 kV/cm. The air-pressure disturbance, lasting tens of microseconds, is recorded using a broadband microphone. The acoustic bandwidth extends from a few Hz to almost 1 MHz. Acoustic spectral components at integer multiples of laser repetition rate (1 kHz) are obtained using harmonics of a lock-in amplifier referencing the synchronized laser output. Measurements at the 100th harmonic (100 kHz) are favorable due to higher signal amplitude and lower ambient noise. The inset of Fig. 8 shows the experimental setup used for detection of THz waves through sound. A pulsed laser and its second harmonic, with adjustable time delay t_R, create a plasma that emits acoustic pulses at the laser repetition rate. This plasma interacts with a THz pulse, with adjustable time delay t_d, and the acoustic amplitude has a linear dependence on the THz intensity (or quadratic dependence on the field) applied to the air-plasma[15].

As in the THz-REEF experiment, free electrons are accelerated or decelerated in the THz field depending on the THz polarity with respect to the electron drift velocity at their time of birth. Monitoring acoustic emission for parallel and antiparallel electron drift velocity reveals the acoustic enhancement from THz-field-accelerated electrons and their energy transfer released in the form of heat. Single-shot acoustic waveforms captured at various distances from the plasma show that even at 11 meters of acoustic propagation (test limit due to lab space), spectral content well into the ultrasonic region is still available for detection[49]. Acoustic measurements do not require direct line of sight, meaning useful data might be collected from an operator behind a barrier, using reflected or transmitted acoustic waves. In addition, the pressure attenuation is $1/r$ with radial distance, whereas the fluorescence intensity decays at $1/r^2$.

Applications

THz radiation generated and detected using laser air photonics remains a relatively young technique, but there exist a wide range of potential applications[50]. Some examples include linear and non-linear THz spectroscopy[51-52], determination of the carrier-envelope (CE) phase of ultra-short (<10 fs) laser pulses[20], identification of materials[53-54], THz-wave polarization control[26,55], plasma diagnostics[56], and remote THz generation and detection[14,29,45].

A THz-ABCD spectrometer using air or select gases as both THz emitter and sensor is capable of measuring material optical properties covering the entire "THz gap" and well beyond, if reflection geometry is used, for solid and liquid materials. In comparison with commonly used detection methods, gases do not exhibit either the phonon absorption seen in EO crystals, or carrier lifetime limitations as observed in photoconductive dipole antennas. Fig. 9 compares absorption spectra of ambient air containing 15 % relative humidity between the air photonic THz-ABCD system and a conventional FTIR system, showing excellent agreement between the methods.

Typically, when performing a spectroscopic measurement, a short pulse of THz radiation containing a broad range of frequencies is allowed to pass through or reflect off a target material. After interaction with the sample, the remaining radiation can be analyzed to determine what frequencies were absorbed during the interaction. It is also possible to extract the index of refraction for the material for this broad range of frequencies in either transmission or reflection geometries with only two measurements (a reference measurement and sample measurement). Once the complex index of refraction is determined, the material's absorption coefficient can be calculated.

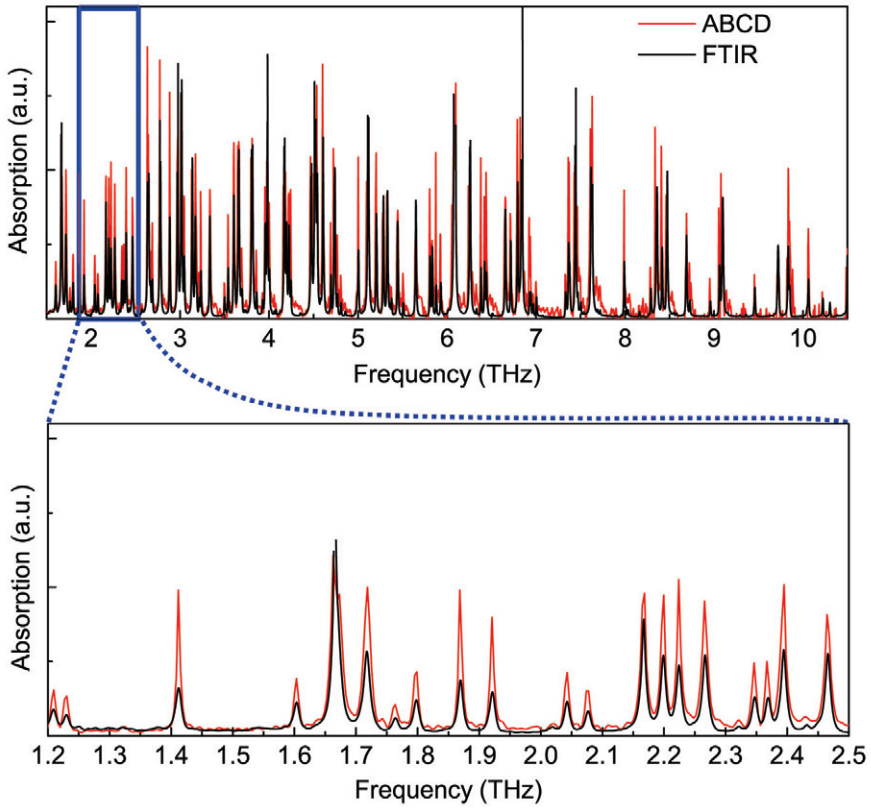

Fig. 9 Spectroscopy data of water vapor absorption for THz-ABCD and FTIR systems. Measurements were independently performed under a relative humidity of 15 %.

Fig. 10a shows a linear spectral measurement of α-BBO in both transmission and reflection modes using a THz-ABCD spectrometer similar to the setup in Fig. 1a[57]. The reference spectrum and transmitted spectra for both the *o* beam and the *e* beam are shown. The transmitted signal level in the range of 5 – 7 THz and above 10 THz for the *o* beam, and above 6 THz for the *e* beam, respectively, is as low as the noise floor due to the large THz wave attenuation by the crystal. Optical properties in these regions can only be revealed by performing measurements in reflection. The reference spectrum covers from 0.3 to over 20 THz with a dip around 18.3 THz due to the two-phonon absorption of the silicon beamsplitter depicted in Fig. 1a. The positions of sharp changes in reflected spectra are coincident with positions of those dips in transmitted spectra. Fig. 10b plots absorption coefficients α_o and α_e and refractive indices n_o and n_e of the α-BBO crystal.

Challenges, limitations, and opportunities

Although laser air photonics technology has opened new possibilities for application, many areas remain for improvement. Remote sensing and standoff detection with THz waves could be considered one of the most challenging topics in THz sensing. Due especially to strong water vapor attenuation in the THz frequency range and insufficient THz power, broadband THz sensing has been limited to short distances (a few centimeters to several meters). The generation of air-plasma near the target(s), through laser excitation, provides one approach to remote detection. The THz-ABCD method offers broadband sensing capabilities, but the THz-induced second harmonic signal cannot be collected from either a backwards or sideways direction. It is also necessary to provide a high voltage local oscillator bias that cannot be readily placed near the remote target for coherent detection.

While remote THz wave generation (> 100 meters) is realistic, coherent remote sensing remains extremely challenging. Currently, the only known solution is to use a two-color laser field to generate air-plasma near the target, measuring THz wave information indirectly through THz-field-induced changes in plasma fluorescence or acoustics. THz air-plasma detection through THz-REEF or TEA, in contrast to nearly all other THz wave sensing methods, enables omnidirectional signal collection, and significantly mitigates the problem of THz absorption by atmospheric moisture. Although both remote generation and detection have been demonstrated separately, it remains to combine these laboratory demonstrations to realize real world THz remote spectroscopy of explosives or other hazardous materials.

Using an intense laser with millijoule pulse energy for many practical applications is also a challenge. The focusing of high intensity optical pulses over long distances with precision, and practical control of the THz amplitude and phase at these ranges has not yet been demonstrated. While some applications such as battlefield monitoring or sensing in

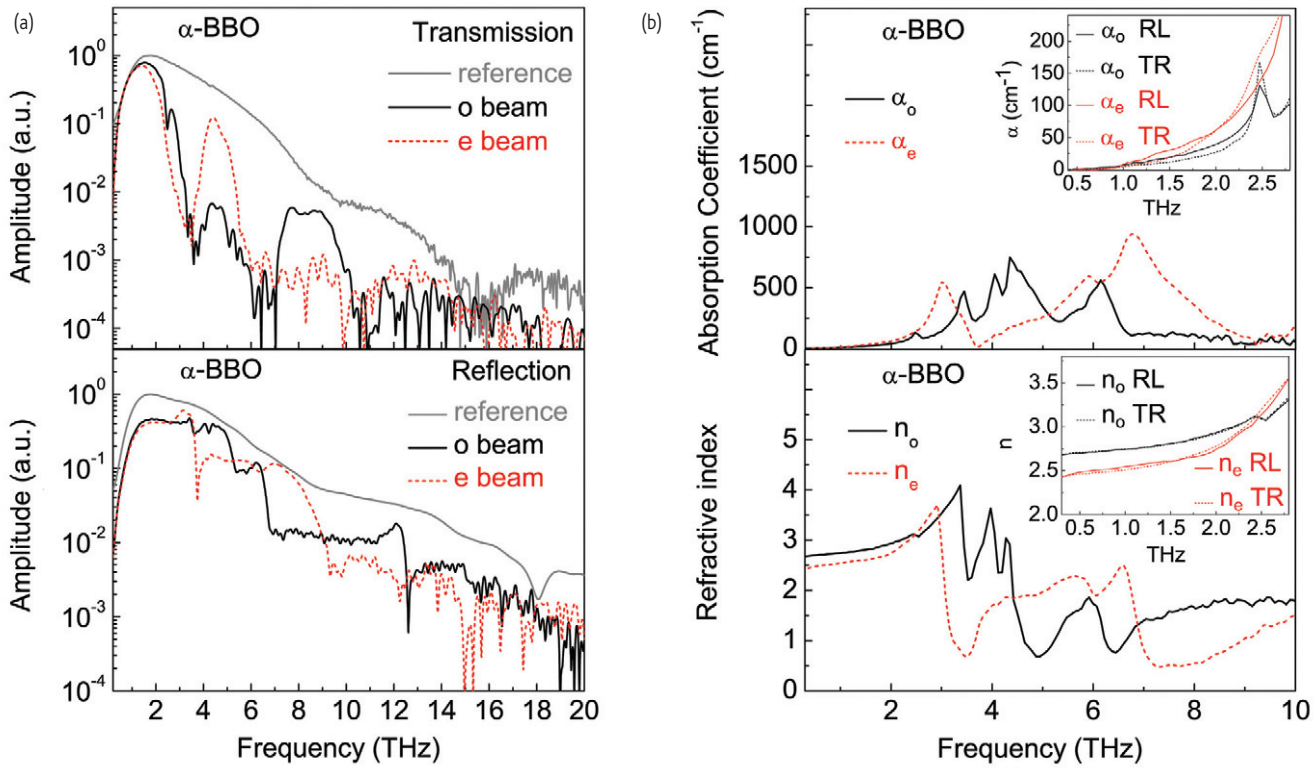

Fig. 10 (a) Measured transmitted and reflected THz spectra of a 0.3 mm-thick α-BBO crystal and reference spectrum. (b) Absorption coefficients and refractive indices of the α-BBO for both e and o crystal axis in the range of 0.3 – 10 THz. (Insets) Comparison between transmission (TR) and reflection (RL) measurements. Reprinted with permission from[61]. © 2009, American Institute of Physics.

remote atmospheric locations may be feasible, public safety must also be considered. These limitations are motivation for improvements to this technology, and/or alternative solutions for remote THz spectroscopy. In the future, we will need to address scientific and technical concerns, provide guidelines and solutions to satisfy safety issues, and develop further approaches that make use of THz wave laser air photonic systems and their unique abilities. As a summary, Table 1 provides some advantages and disadvantages associated with air photonics for THz wave generation and detection.

Outlook and future perspectives

Laser air photonics for THz wave technology remains an active area of research both scientifically and for practical uses, particularly geared towards sensing, identification, and materials characterization. A further understanding of the science behind THz wave generation and detection mechanisms in laser-induced gas-plasmas is crucial to advancements in THz wave sources and sensors. Many parameters influence THz wave generation, manipulation, and detection, such as: optical energy, pulse duration, beam polarization, optical phase (in dual color excitation), plasma density, beam divergence angle, air turbulence, air density, and humidity. The study of THz wave generation and detection using lasers with higher powers and shorter pulse durations will push the envelope for THz field strengths and bandwidths. The success of the broader impact of the sensor will come through the five S's: sensitivity, selectivity, simplicity, scalability, and stability. By focusing on these challenges, key applications in spectroscopy, non-invasive evaluation of materials, and imaging will continue to flourish. THz air-plasma systems are expected to provide orders of magnitude improvement in field strength, bandwidth,

Table 1 Advantages and disadvantages of laser air photonics for THz wave generation and detection

Advantages	Disadvantages
Emitter and sensor can be ambient air	Intense laser pulses are needed
Capable of MV/cm peak electric field strengths	Low optical-to-THz conversion efficiency
> 100 THz bandwidths	Bulky, amplified laser systems required
Sensor does not suffer from phonon absorption	Intense optical radiation is not eye-safe
Emitter and sensor can be formed remotely	Critical alignment is necessary
THz can be detected through fluorescence or acoustic wave modulation	Lower sensitivity from the use of high-order nonlinearity

and sensitivity over commercial THz time-domain spectrometer (THz-TDS) systems available today. For example, recent progress in laser air photonics shows that a bandwidth covering the entire "THz gap," and continuously stretching to the near-IR can be obtained[58].

In the future, laser air photonics may find alternative niche applications. The following "wish list" items may provide useful topics of study:

- Using compact oscillator lasers to replace amplified lasers for THz-ABCD
- Selecting alternative gases to increase generation and detection efficiency
- Studying plasma sensors for detecting other forms of electromagnetic radiation such as UV, microwave, x-rays, or gamma rays

Recent observations that THz radiation is able to modulate both the fluorescence and acoustics of laser-induced plasma in air, means that THz-REEF or TEA not only present feasible solutions toward remote THz wave detection, but also open exciting new areas of basic research. The fluorescence technique could, for example, exploit the Stark effect to directly measure rectified THz fields inside of a filament core, providing evidence of potentially enormous field strengths that are unable to couple out into free space. Furthermore, acoustic techniques could make it possible to study solids or liquids with high absorption coefficients by indirectly studying changes in a sample's acoustic properties under illumination of high-field THz radiation. It is clear that pioneering direction, and growth in application, will require continued advances in laser air photonics technology. mt

Acknowledgements

This work was supported in part by the U.S. Office of Naval Research (ONR), the Defense Threat Reduction Agency (DTRA), National Science Foundation (NSF) under Grant No. 0333314, ALERT, and the U.S. Department of Homeland Security through the DHS-ALERT Center under Award No. 2008-ST-061-ED0001. The views and conclusions contained in this document are those of the authors and should not be interpreted as necessarily representing the official policies, either expressed or implied, of the U.S. Department of Homeland Security. The authors gratefully acknowledge assistance from Dr. Nicolas Karpowicz, Dr. Jingle Liu, Dr. Xaofei Lu, Dr. Karen Ho, and Dr. David Brigada.

REFERENCES

1. Boyd, G., *Engineering and Science* (1958) **22**(2), 34.
2. Maker, P. D., *et al.*, 3rd International Conference ed.; Columbia University Press, Paris, (1963), Vol. 2, pp 1559.
3. Strickland, D., and Mourou, G., *Opt Communs* (1985) **55**(6), 447.
4. Hamster, H., *et al.*, *Phys Rev Lett* (1993) **71**(17), 2725.
5. Cook, D. J., and Hochstrasser, R. M., *Opt Lett* (2000) **25**(16), 1210.
6. Bartel, T., *et al.*, *Opt Lett* (2005) **30**(20), 2805.
7. Kress, M., *et al.*, *Opt Lett* (2004) **29**(10), 1120.
8. Löffler, T., *et al.*, *Acta Phys Pol A* (2005) **107**, 99.
9. Roskos, H. G., *et al.*, *Laser Photon Rev* (2007) **1**(4), 349.
10. Tzortzakis, S., *et al.*, *Opt Lett* (2002) **27**(21), 1944.
11. Dai, J., *et al.*, *Phys Rev Lett* (2006) **97**(10), 103903.
12. Karpowicz, N., *et al.*, *Appl Phys Lett* (2008) **92**(1), 011131.
13. Liu, J., and Zhang, X. C., *Phys Rev Lett* (2009) **103**(23), 235002.
14. Liu, J., *et al.*, *Nat Photon* (2010) **4**(9), 627.
15. Clough, B., *et al.*, *Opt Lett* (2010) **35**(21), 3544.
16. Clough, B., *et al.*, *Opt Lett* (2011) **36**(13), 2399.
17. Liu, J., *et al.*, *Phys Rev E* (2010) **82**(6), 066602.
18. Liu, J., and Xi-Cheng, Z., *EEE J Sel Quant Elec* (2011) **17**(1), 229.
19. Xie, X., *et al.*, *Phys Rev Lett* (2006) **96**(7), 75005.
20. Kresz, M., *et al.*, *Nat Phys* (2006) **2**(5), 327.
21. Kim, K.-Y., *et al.*, *Opt Express* (2007) **15**(8), 4577.
22. Kim, K. Y., *et al.*, *Nat Photon* (2008) **2**(10), 605.
23. Zhang, Y., *et al.*, *Opt Express* (2008) **16**(20), 15483.
24. Houard, A., *et al.*, *Phys Rev Lett* (2008) **100**(25), 255006.
25. Wen, H., and Lindenberg, A. M., *Phys Rev Lett* (2009) **103**(2), 023902.
26. Dai, J., *et al.*, *Phys Rev Lett* (2009) **103**(2), 023001.
27. Karpowicz, N., and Zhang, X. C., *Phys Rev Lett* (2009) **102**(9), 093001.
28. Liu, J., and Zhang, X. C., *Phys. Rev. Lett.* (2009) **103**, 235002.
29. Wang, T. J., *et al.*, *Appl Phys Lett* (2010) **97**, 111108.
30. Dai, J., *et al.*, *Phys Rev Lett* (2006) **97**(10), 103903.
31. Lu, X., *et al.*, *Appl Phys Lett* (2008) **93**, 261106.
32. Ho, I., *Opt Express* (2010) **18**(3), 2872.
33. Karpowicz, N., and Zhang, X. C., *Phys Rev Lett* (2009) **102**(9), 093001.
34. Kim, K. Y., *et al.*, *Opt Express* (2007) **15**(8), 4577.
35. Silaev, A., and Vvedenskii, N., *Physica Scripta* (2009) **2009**, 014024.
36. Wu, H. C., *et al.*, *New J Phys* (2008) **10**, 043001.
37. Xu, J., and Zhang, X. C., *Introduction to THz Wave Photonics*. Springer: 2010.
38. Wu, Q., and Zhang, X. C., *Appl Phys Lett* (1995) **67**, 3523.
39. Jepsen, P. U., *et al.*, *Phys Rev E* (1996) **53**(4), R3052.
40. Nahata, A., *et al.*, *Appl Phys Lett* (1996) **68**, 150.
41. Thomson, M. D., *et al.*, *Opt Express* (2010) **18**(22), 23173.
42. Cook, D., *et al.*, *Chem Phys Lett* (1999) **309**(3-4), 221.
43. Nahata, A., and Heinz, T. F., *Opt letters* (1998) **23**(1), 67.
44. Shelton, D. P., *Phys Rev A* (1990) **42**(5), 2578.
45. Dai, J., and Zhang, X. C., *Appl Phys Lett* (2009) **94**(2), 021117.
46. Dai, J., *et al.*, *IEEE T Terahertz Sci Technol* (2011) **1**(1), 274.
47. Radziemski, L. J., *et al.*, *Anal Chem* (1983) **55**(8), 1246.
48. Sobral, H., *et al.*, *Appl Phys Lett* (2000) **77**(20), 3158.
49. Clough, B., *et al.*, *Proc of SPIE* (2011) **7938**, 793804.
50. Ferguson, B., and Zhang, X.-C., *Nat Mater* (2002) **1**(1), 26.
51. Gaal, P., *et al.*, *Phys Rev Lett* (2006) **96**(18), 187402.
52. Ho, I. C., and Zhang, X. C., *Appl Phys Lett* (2011) **98**, 241908.
53. Chen Y, *et al.*, *Proc SPIE* (2004) **5411**, 1.
54. Chen, J., *et al.*, *Opt. Express* (2007) **15**(19), 12060.
55. Wen, H., and Lindenberg, A. M., *Phys Rev Lett* (2009) **103**, 023902.
56. Liu, J., and Zhang, X. C., *Appl Phys Lett* (2010) **96**(4), 041505.
57. Liu, J., and Zhang, X., *J Appl Phys* (2009) **106**(2), 023107.
58. Matsubara, E., and Ashida, M., *35th IRMMW* Houston TX, USA, 2011.
59. Xie, X., *et al.*, *Phys Rev Lett* (2006) **96**, 075005.
60. Dai, J., *et al.*, *IEEE J Sel Top Quant* (2011) **17**, 183.
61. Liu, J. and Zhang, X. C., *J Appl Phys* (2009) **106**, 023107.